RSC Advances

PAPER

View Article Online
View Journal | View Issue

Cite this: *RSC Adv.*, 2021, **11**, 22273

The discovery of new phloroglucinol glycosides from *Agrimonia pilosa* and the mechanism of oxidative dearomatization of the methyl-substituted phloroglucinol derivatives†

Jia Zhang, Ya-Nan Yang, Jian-Shuang Jiang, Zi-Ming Feng, Xiang Yuan, Xu Zhang and Pei-Cheng Zhang *

Received 8th May 2021
Accepted 15th June 2021

DOI: 10.1039/d1ra03588f

rsc.li/rsc-advances

Six methyl-substituted phloroglucinol glycosides (**1–6**) were isolated from *Agrimonia pilosa*, including four new compounds (**1–3**, **6**). The aglycones (**1a–4a**) of **1–4** and their corresponding oxidized products (**1c–4c**) were also obtained from *A. pilosa*. The structures were determined by a series of spectroscopic analyses and chiral separation. Notably, the structures of aglycones **1a–4a** were unstable and prone to oxidation spontaneously, to yield the dearomatized structures **1c–4c**. The mechanism of oxidative dearomatization was disclosed as a free-radical chain reaction with $^3O_2$ by the techniques of HPLC-HR-MS^2, EPR spectra and DFT-calculation, and hydroperoxide was defined as the intermediate.

Introduction

Agrimonia pilosa is a plant in the Rosaceae family that is mainly distributed throughout East Asia. As a traditional Chinese medicine, the herbs of *A. pilosa* have been used to treat malaria, bleeding, dysentery and debility for many years.[1] The chemical investigation of *Agrimonia pilosa* suggested the presence of phloroglucinols in various forms, such as the dimer agrimophol, with significant antituberculosis activity.[2] During the phytochemical research on *A. pilosa*, six dimethyl-substituted phloroglucinol glycosides (**1–6**), four of their aglycones (**1a–4a**), and four pairs of dearomatized products (**1c–4c**) were isolated (Fig. 1). Compounds **1–3** and **6** are new phloroglucinol glycosides. However, there is an inescapable problem in which aglycones **1a–4a** are readily oxidized by air to form the dearomatized products **1c–4c** spontaneously.

Reference surveys revealed that the natural dearomatized phloroglucinol derivatives display remarkable pharmacological activities. α-Acids, isolated from hop (*Humulus lupulus* L.), showed antimetabolic activities,[3] and hydroxysafflor yellow A (HSYA), isolated from *Carthamus tinctorius*,[4] exhibited cardiovascular effects.[5] Over the past few years, the dearomatization of isopentenyl- and *C*-glucosyl-substituted phloroglucinols has attracted much attentions from synthetic chemists. Most dearomatizations were proceed by oxidation under alkaline environment. The oxidants include lead(II) acetate trihydrate,[6] [bis(trifluoroacetoxy)iodo]benzene,[7] *tert*-butylhydroperoxide,[8] and oxygen.[9] Meanwhile, sodium hydride,[10] sodium bicarbonate,[7] sodium hydroxide,[8] and pyridine[9] were utilized as alkaline. In 2019, our group employed ammonium chloride and ammonia buffer salt as alkaline to achieve the oxidative dearomatization of di-*C*-glucosyl-substituted phloroglucinols.[11] While the mechanism of oxidative dearomatization on

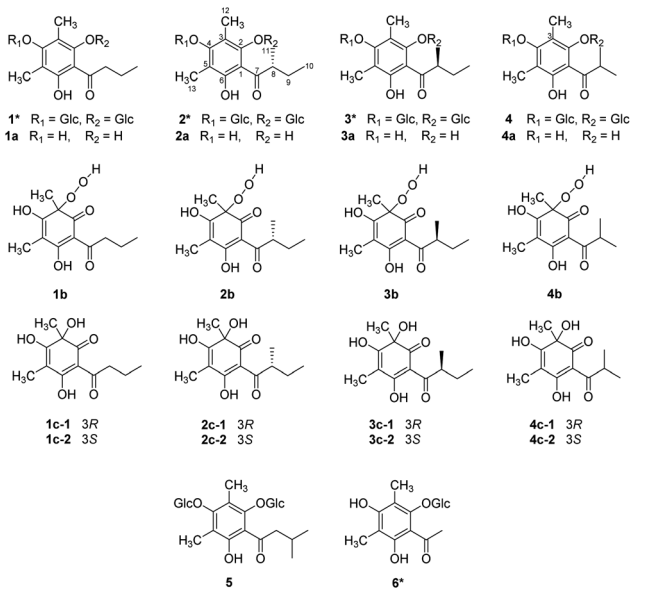

Fig. 1 Chemical structures of compounds **1–6**.

State Key Laboratory of Bioactive Substance and Function of Natural Medicines, Institute of Materia Medica, Peking Union Medical College, Chinese Academy of Medical Sciences, Beijing 100050, People's Republic of China. E-mail: pczhang@imm.ac.cn

† Electronic supplementary information (ESI) available: Structural elucidations of **1** and **6**, general experimental procedure, HPLC-MS^2 analysis, DFT calculation details, UV, IR, NMR, and HRESIMS spectra. See DOI: 10.1039/d1ra03588f

phloroglucinol by oxygen were barely studied, the phenomenon of auto oxidative dearomatization of **1a–4a** inspired us to explore the in-depth mechanism. Consequently, a free-radical chain mechanism was determined by the techniques of HPLC-HR-MS^2, EPR (electroparamagnetic resonance) spectra, and DFT calculations.

Results and discussion

The structures and absolute configurations of **2** and **3** were elucidated by extensive spectroscopic data (Tables S1 and S2†) and a chiral separation method. Of note is that **2** and **3** are a pair of epimers with the opposite chirality at C-8, sharing the same molecular formula of $C_{25}H_{38}O_{14}$ by HR-ESI-MS. The ^{1}H NMR spectrum of **2** exhibited two aliphatic methyl groups at δ_H 0.97 (3H, t, J = 7.5 Hz) and 1.00 (3H, d, J = 7.5 Hz), two aromatic methyl groups at δ_H 2.20 and 2.32 (each 3H, s), one methylene group at δ_H 1.42 and 1.91 (each 1H, m), one methine group at δ_H 3.74 (1H, overlapped), and two anomeric protons of the β-glucopyranosyl moiety at δ_H 4.43 and 4.67 (each 1H, J = 7.5 Hz). The ^{13}C NMR spectrum of **2** displayed twenty-five carbon resonances, including the characteristic signals of two glucopyranosyl moieties and one phloroglucinol.

The ^{1}H–^{1}H COSY correlations between H_3-11 and H-8, H-8 and H_2-9, and H_2-9 and H_3-10 implied the presence of the H_3-11–H-8–H_2-9–H_3-10 proton spin system, corresponding to an α-methylbutyryl group. This was further verified by the HMBC correlations from H-8 to C-7/C-9/C-10/C-11, from H_3-10 to C-8/C-9, and from H_3-11 to C-7/C-8/C-9. The HMBC correlations from H-1′ to C-2 and from H-1″ to C-4 placed two glucopyranosyl moieties at C-2 and C-4. In addition, HMBC correlations from H_3-12 to C-2/C-3/C-4 and from H_3-13 to C-4/C-5/C-6, suggested two aromatic methyl groups were located at C-3 and C-5, respectively (Fig. 2A). The configuration of two glucopyranosyl moieties were determined as β-D based on the $^3J_{1',2'}$, $^3J_{1'',2''}$ values (7.5 Hz) and the retention time (20.39 min) by GC analyses (Fig. S2 and S3†). Hence, the structure of **2** was deduced as 3,5-dimethyl-α-methylbutyrylphloroglucinol-2,4-*O*-β-D-diglucopyranoside.

The 1D and 2D NMR data of **3** were in good agreement with those of **2**, except for the difference of the α-methylbutyryl group signals. Compared with ^{1}H NMR spectrum of **2**, the chemical shifts of H-9a, H-9b and H_3-10 of **3** were shifted upfield by 0.38, 0.12, and 0.23 ppm, while the chemical shift of H_3-11 of **3** was shifted downfield by 0.13 ppm. Detailed analysis of the NMR data revealed that the planar structure of **3** was identical with **2** but the opposite chirality at C-8, resulting in a pair of epimers.

Initially, the ECD spectra were expected to determine the absolute configuration of C-8, but the experimental ECD spectra of **2** and **3** were very similar, suggesting the ECD cotton effects were mainly affected by glucopyranosyl moieties (Fig. 2B). To determine the absolute configuration of C-8, (*S*)-aglycone **3a** was synthesized from phloroglucinol through a series of chemical reactions (Section S3.6†), and compounds **2** and **3** were hydrolyzed by 2 M HCl at 60 °C (Section S3.4†). The products of the acidic hydrolysis were analyzed by a normal-phase chiral chromatographic column, and the unequal enantiomers **2a** and **3a** were monitored (Fig. 2C). This is due to the fact that carbonyl tautomerism occurred in the acidic hydrolysis of **2** and **3**. However, the area ratios of the two peaks 0.9 : 1 in **2** and 1 : 0.8 in **3** suggested that the absolute configurations of C-8 in **2** and **3** were *R* and *S*, respectively.

The structures of **1** and **6** were also identified as new compounds (Section S1†), **4** and **5** were elucidated as kunzeaphlogin F and D, respectively.[12]

Apart from the phloroglucinol glucosides, a series of dimethyl-substituted phloroglucinol derivatives **1a–4a** and **1c–4c** were also isolated (Section S2†). During the separation of **1a–4a**, it's interesting to find that when the mixture of **1a–4a** was stored at methanol under room temperature, new peaks **1b–4b**, **1c** and **4c** were monitored by HPLC analyses after eight days (Fig. 3A). As time went on, peaks **1b–4b** were disappeared and peaks **1c–4c** were increased a lot after 6 months (Fig. 3A).

The structures of **1c–4c** have been elucidated as the dearomatized products of **1a–4a** (Fig. 1), but **1b–4b** can't be isolated

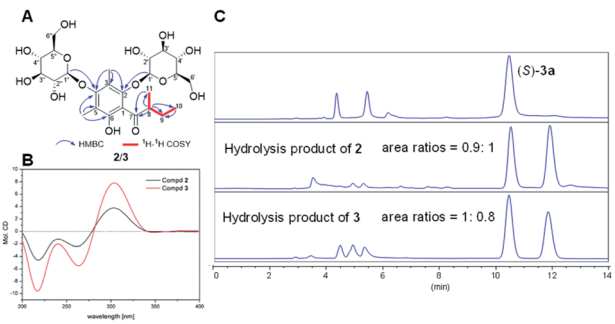

Fig. 2 (A) Key HMBC and COSY correlations of **2** and **3**; (B) experimental ECD spectra of **2** and **3**; (C) HPLC-DAD spectra of (*S*)-**3a**, hydrolysis products of **2** and **3** (HPLC condition: CHIRALPAK AD-H, 250 × 4.6 mm, *n*-hexane: IPA = 90 : 10, T = 40 °C, v = 1 mL min^{-1}, λ = 280 nm).

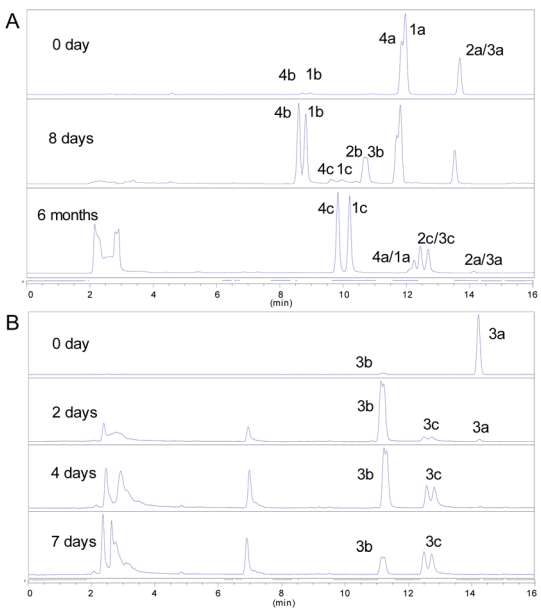

Fig. 3 (A) HPLC-DAD spectra of **1a–4a**; (B) HPLC-DAD spectra of 0.05 M (*S*)-aglycone **3a**. (HPLC condition: 0–16 min, 35–70% MeCN–H_2O, T = 40 °C, v = 1 mL min^{-1}, λ = 254 nm).

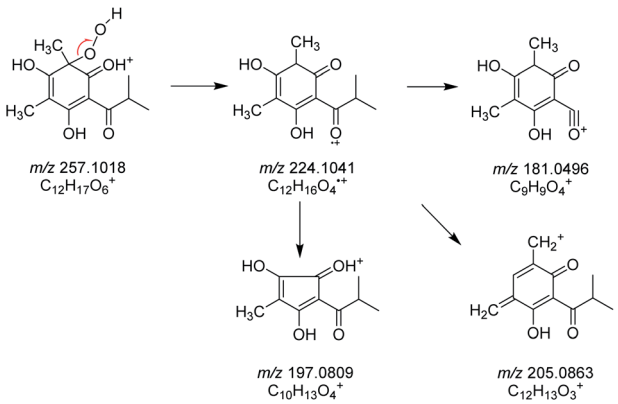

Scheme 1 The main fragmentation pathway of **4b**.

purely due to their poor stability. Therefore, high performance liquid chromatography (HPLC)-high resolution tandem mass spectrometry (HR-MS^2) was applied for elucidating the structures of **1b–4b** (Section S4†). For example, **4b** were diagnosed as hydroperoxide by the high resolution quasi-molecular ions *m*/*z* 257.1018 and main fragment ions *m*/*z* 224.1041, 205.0863, 197.0809, 181.0496 (Scheme 1). Subsequently, 0.05 M synthesized (*S*)-aglycone **3a** was stored at oxygen-saturated methanol under room temperature and monitored by HPLC every two days. The results indicated that **3a** first rapidly transformed into **3b** and then **3b** transformed into **3c** gradually (Fig. 3B). Those findings support the conclusion that dimethyl-substituted phloroglucinol derivatives can transform into the dearomatized structures spontaneously, and the hydroperoxides acted as the intermediate.

Some mechanisms of oxidative dearomatization, such as Diels–Alder reactions, [2 + 2] cycloaddition, or free-radical reaction, have been introduced before,[13] and singlet oxygen was often applied as the oxygen donor. But when we add TEMP (2,2,6,6-tetramethylpiperidine) to the reaction system of **4a** for detecting singlet oxygen, the EPR spectra didn't showed the signal of the adduct of TEMP and singlet oxygen (Fig. S6†), indicating oxygen participating in the reaction was the triple

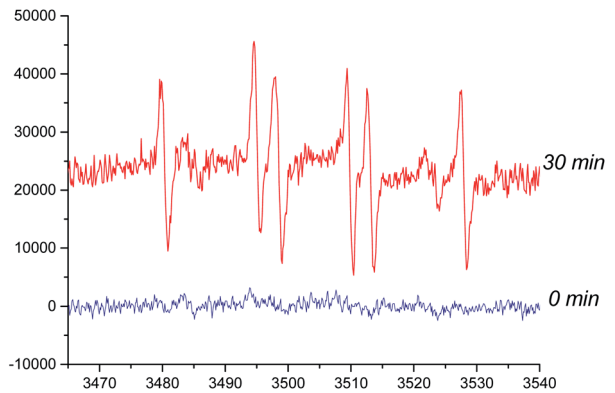

Fig. 4 Electroparamagnetic resonance (EPR) spectra of **4a** (room temperature in oxygen-saturated acetonitrile). The concentrations of DMPO and **4a** were 500 and 50 mmol L^{-1}, respectively.

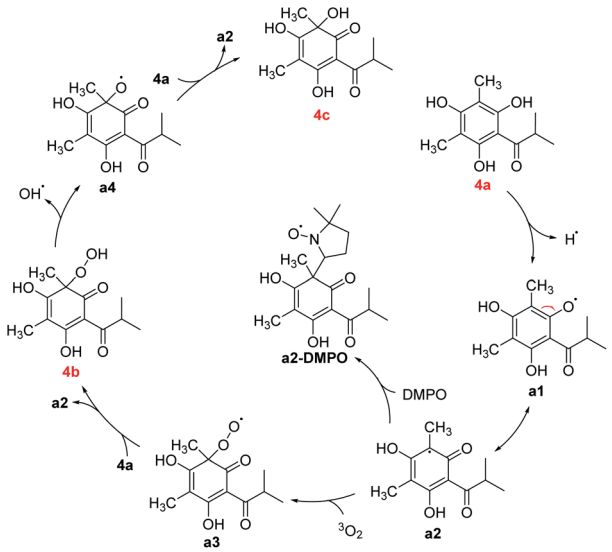

Scheme 2 Proposed mechanism of oxidative dearomatization of **4a**.

state ($^3O_2$) instead of singlet state ($^1O_2$). To further explore the mechanism, DMPO (5,5-dimethyl-1-pyrroline *N*-oxide) was employed as a spin trapper and monitored by HPLC, the oxidative dearomatization was prevented (Fig. S7 and S8†). Obviously, the oxidative dearomatization of **4a** involves a radical intermediate. Furthermore, the characteristic signal of the adduct of alkyl radical (R$^\bullet$) and DMPO in the EPR spectra (Fig. 4) suggested that the oxidative dearomatization of **4a** is a free-radical reaction. Based on the above HPLC and EPR results, the free-radical mechanism for **4a** were proposed as Scheme 2. Firstly, **4a** lose a hydrogen atom and give the radical **a1**. Because **a1** and **a2** were a pair of resonance structures, **a1** can transform into **a2**. Then, radical **a2** react with oxygen to give the peroxy radical **a3**, followed by the hydrogen atom transfer from **4a**, giving the intermediate **4b**. In the next step, the hydroperoxide **4b** transform into the oxygen free-radical **a4** and hydroxyl radical ($^\bullet$OH) through the homolysis of peroxy bond. Finally, the oxygen radical **a4** captures hydrogen atom of **4a** to gain the dearomatized product **4c**. As the chain carrier, radical **a2** was considered as the alkyl radical trapped by DMPO.

Density functional theory (DFT) research was performed to better understand the mechanisms, the Gibbs free energy profile was established as shown in Fig. 5. The transition states of the reactions of **a2** and $^3O_2$, **a3** and **4a**, **a4** and **4a** were defined as TS-**1–3**, respectively. Firstly, the Gibbs free energy barrier for the electrophilic addition of radical **a2** to $^3O_2$ was 17.7 kcal mol^{-1}, and the relative energy of **a3** was 6.7 kcal mol^{-1}. Likewise, when the radical peroxy radical captures the hydrogen atom of **4a**, exhibiting a similar relative energy barrier 17.0 kcal mol^{-1}, but the relative energy of product was −26.6 kcal mol^{-1}, leading the production of the intermediate **4b**. In fact, the rate of generating **4b** was faster than **4c**, but it still needs two days to achieve, which accord with the calculated energy barriers (17.7 and 17.0 kcal mol^{-1}). There is no transition state during the homolysis of O–O bond, proved by the potential energy surface scanning (Fig. S12†). The BDE of O–O bond was calculated as

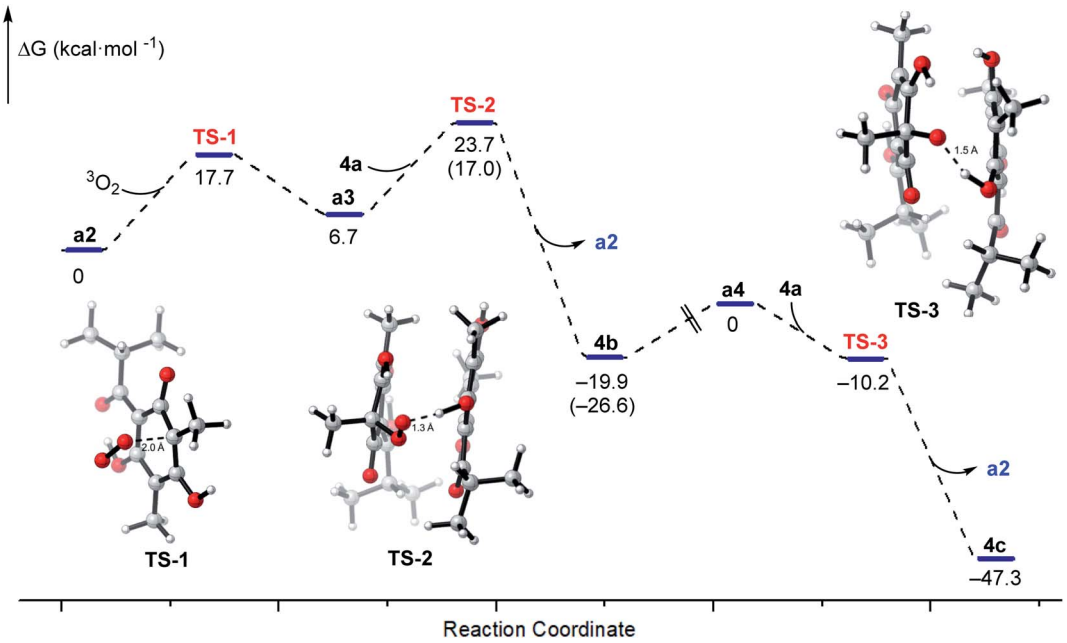

Fig. 5 Gibbs free energy profiles for the free-radical chain reaction of **4a** and the structures of transition states TS-**1**–**3**.

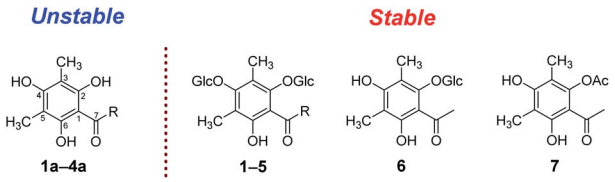

Fig. 6 Stability of the substituted phloroglucinol derivatives (R = *n*-propyl, isopropyl, isobutyl).

45.3 kcal mol $^{-1}$, indicating the cleavage of O–O bond was the rate-limiting step, which was also correspond to the slow generation of **4c** from **4b**. Besides, the process from **a4** to **4c** was barrier-less, the relative energy of TS-**3** and the product **4c** were −10.2 and −47.3 kcal mol $^{-1}$. Generally, the auto oxidative dearomatization pathway of dimethyl-substituted phloroglucinol derivatives were kinetically and thermodynamically accomplished.

When the 2-hydroxyl of the phloroglucinol derivatives get glycosylation or esterification, such as **1**–**7** (Fig. 6), the structures couldn't transform into the hydroperoxides or dearomatized structures. Structurally, two free phenolic hydroxyls at C-2 and C-6 were essential for the auto oxidative dearomatization, one hydroxyl formed a strong hydrogen bond with the carbonyl, and another hydroxyl was regarded as the hydrogen atom donor attributed to the radicals.

Conclusions

As a research hot spot, studies of phloroglucinol derivatives have been ongoing for many years. In present study, fortunately, six phloroglucinol glucosides (**1**–**6**), together with four aglycones (**1a**–**4a**) and four pairs of dearomatized products (**1c**–**4c**) were isolated from *A. pilosa*. Moreover, this is the first report on the instability and structural variability of dimethyl-substituted phloroglucinol derivatives. We found that dimethyl-substituted phloroglucinol derivatives were readily oxidized to their dearomatized structures, and the intermediates were determined as hydroperoxides by HPLC-HR-MS^2. With the aid of EPR and DFT calculations, the mechanism was clarified as a free-radical chain reaction.

Conflicts of interest

There are no conflicts to declare.

Acknowledgements

The project was financially supported by the Chinese Academy of Medical Sciences (CAMS) Initiative for Innovative Medicine (No. 2019-I2M-1-005).

Notes and references

1 (*a*) H. Kato, W. Li, M. Koike, Y. H. Wang and K. Koike, Phenolic glycosides from *Agrimonia pilosa*, *Phytochemistry*, 2010, **71**, 1925–1929; (*b*) H. W. Kim, J. Park, K. B. Kang, T. B. Kim, W. K. Oh, J. Kim and S. H. Sung, Acylphloroglucinolated catechin and phenylethyl isocoumarin derivatives from *Agrimonia pilosa*, *J. Nat. Prod.*, 2016, **79**, 2376–2383; (*c*) D. H. Nguyen, U. M. Seo, B. T. Zhao, D. D. Le, S. H. Seong, J. S. Choi, B. S. Min and M. H. Woo, Ellagitannin and flavonoid constituents from *Agrimonia pilosa* Ledeb. with their protein tyrosine phosphatase and acetylcholinesterase inhibitory activities, *Bioorg. Chem.*, 2017, **72**, 293–300.

2 (*a*) N. Zhao, M. N. Sun, K. Burns-Huang, X. J. Jiang, Y. Ling, C. Darby, S. Ehrt, G. Liu and C. Nathan, Identification of Rv3852 as an agrimophol-binding protein in *Mycobacterium tuberculosis*, *PLoS One*, 2015, **10**, e0126211; (*b*) J. Wu, R. Mu, M. N. Sun, N. Zhao, M. M. Pan, H. S. Li, Y. Dong, Z. G. Sun, J. Bai, M. W. Hu, C. F. Nathan, B. Javid and G. Liu, Derivatives of natural product agrimophol as disruptors of intrabacterial pH homeostasis in *Mycobacterium tuberculosis*, *ACS Infect. Dis.*, 2019, **5**, 1087–1104.

3 M. Van Cleemput, K. Cattoor, K. De Bosscher, G. Haegeman, D. De Keukeleire and A. Heyerick, Hop (*Humulus lupulus*)-derived bitter acids as multipotent bioactive compounds, *J. Nat. Prod.*, 2009, **72**, 1220–1230.

4 Z. M. Feng, J. He, J. S. Jiang, Z. Chen, Y. N. Yang and P. C. Zhang, NMR solution structure study of the representative component hydroxysafflor yellow A and other quinochalcone *C*-glycosides from *Carthamus tinctorius*, *J. Nat. Prod.*, 2013, **76**, 270–274.

5 (*a*) X. Bai, W. X. Wang, R. J. Fu, S. J. Yue, H. Gao, Y. Y. Chen and Y. P. Tang, Therapeutic potential of hydroxysafflor yellow A on cardio-cerebrovascular diseases, *Front. Pharmacol.*, 2020, **11**, 01265; (*b*) Y. Sun, D. P. Xu, Z. Qin, P. Y. Wang, B. H. Hu, J. G. Yu, Y. Zhao, B. Cai, Y. L. Chen, M. Lu, J. G. Liu and X. Liu, Protective cerebrovascular effects of hydroxysafflor yellow A (HSYA) on ischemic stroke, *Eur. J. Pharmacol.*, 2018, **818**, 604–609.

6 M. R. Cann, A. M. Davis and P. V. R. Shannon, The synthesis of some novel deoxyhumulone analogues. Observations on the air-oxidation of 2′,4′,6′-trihydroxy-3′-isopentyl-5′-(3-methylbut-2-enyl)isovalerophenone and its corresponding humulone derivatives, *J. Chem. Soc., Perkin Trans. 1*, 1984, 1413–1421.

7 T. Hayashi, K. Ohmori and K. Suzuki, Synthetic study on carthamin: problem and solution for oxidative dearomatization approach to quinol *C*-glycoside, *Synlett*, 2016, **27**, 2345–2351.

8 E. Collins and P. V. R. Shannon, Dimethylallylation products of phloroacetophenone; a convenient one-stage synthesis of deoxyhumulones, *J. Chem. Soc., Perkin Trans. 1*, 1973, 419–424.

9 (*a*) S. Sato, T. Nojiri and J. I. Onodera, Studies on the synthesis of safflomin-A, a yellow pigment in safflower petals: oxidation of 3-*C*-β-D-glucopyranosyl-5-methylphloroacetophenone, *Carbohydr. Res.*, 2005, **340**, 389–393; (*b*) T. Suzuki, M. Ishida, T. Kumazawa and S. Sato, Oxidation of 3,5-di-*C*-(per-*O*-acetylglucopyranosyl) phloroacetophenone in the synthesis of hydroxysafflor yellow A, *Carbohydr. Res.*, 2017, **448**, 52–56.

10 (*a*) S. Sato, T. Kumazawa, H. Watanabe, K. Takayanagi, S. Matsuba, J. I. Onodera, H. Obara and K. Furuhata, Synthesis of carthamin acetate, the red pigment in safflower petals, *Chem. Lett.*, 2001, **30**, 1318–1319; (*b*) S. Sato, H. Obara, T. Kumazawa, J. I. Onodera and K. Furuhata, Synthesis of (+),(−)-model compounds and absolute configuration of carthamin; a red pigment in the flower petals of safflower, *Chem. Lett.*, 1996, **25**, 833–834; (*c*) H. Obara, S. Namai and Y. Machida, Synthesis of 2-[[3-hydroxy-S-[3-(4-hydroxyphenyl)-1-oxo-2-propenyl]-3-methyl-2,4,6-trioxocyclohex-1-yl]methylene]-4-hydroxy-6-[3-(4-hydroxyphenyl)-1-oxo-2-prophenyl]-4-methyl-1,3,5-trioxocyclohexane, an analog of carthamin, *Chem. Lett.*, 1986, **15**, 495–496.

11 W. Gao, Z. Chen, Y. N. Yang, J. S. Jiang, Z. M. Feng, X. Zhang, X. Yuan and P. C. Zhang, Base-catalyzed oxidative dearomatization of multisubstituted phloroglucinols: an easy access to *C*-glucosyl 3,5,6-trihydroxycyclohexa-2,4-dienone derivatives, *Carbohydr. Res.*, 2019, **484**, 107756.

12 N. Kasajima, H. Ito, T. Hatano and T. Yoshida, Phloroglucinol diglycosides accompanying hydrolyzable tannins from *Kunzea ambigua*, *Phytochemistry*, 2008, **69**, 3080–3086.

13 (*a*) A. A. Ghogare and A. Greer, Using singlet oxygen to synthesize natural products and drugs, *Chem. Rev.*, 2016, **116**, 9994–10034; (*b*) Q. J. Song, T. Niu and H. J. Wang, Theoretical study of the reaction of 2,4-dichlorophenol with $^1O_2$, *J. Mol. Struct.: THEOCHEM*, 2008, **861**, 27–32; (*c*) S. Barradas, G. Hernandez-Torres, A. Urbano and M. C. Carreno, Total synthesis of natural *p*-quinol cochinchinenone, *Org. Lett.*, 2012, **14**, 5952–5955.